Scaling behavior of the terminal transient phase

Thomas Lilienkamp[1,2,*] and Ulrich Parlitz[1,2,3]

[1]*Max Planck Institute for Dynamics and Self-Organization, Am Fassberg 17, 37077 Göttingen, Germany*

[2]*Institute for Nonlinear Dynamics, University of Göttingen, Friedrich-Hund-Platz 1, 37077 Göttingen, Germany*

[3]*DZHK (German Centre for Cardiovascular Research), partner site Göttingen, Robert-Koch-Straße 42a, 37075 Göttingen, Germany*

(Received 5 June 2018; published 20 August 2018)

Transient chaos can emerge in a variety of diverse systems, e.g., in chemical reactions, population dynamics, neuronal activity, or cardiac dynamics. The end of the chaotic episode can either be desired or not, depending on the specific system and application. In both cases, however, a prediction of the end of the chaotic dynamics is required. Despite the general challenges of reliably predicting chaotic dynamics for a long time period, the recent observation of a "terminal transient phase" of chaotic transients provides new insights into the transition from chaos to the subsequent (nonchaotic) regime. In spatially extended systems and also low-dimensional maps it was shown that the structure of the state space changes already a significant amount of time before the actual end of the chaotic dynamics. In this way, the terminal transient phase provides the conceptual foundation for a possible prediction of the upcoming end of the chaotic episode a significant amount of time in advance. In this study, we strengthen the general validity of the terminal transient phase by verifying its existence in another spatially extended model (Gray-Scott model) and the Hénon map, where in the latter case the underlying mechanisms can be understood in an intuitive way. Furthermore, we show that the temporal length of the terminal transient phase remains approximately constant, when changing the system size (Gray-Scott) or parameters (Hénon map) of the investigated models, although the average lifetime of the observed chaotic transients sensitively depends on these variations. Since the timescale of the terminal transient phase is in this sense relatively robust, this insight might be essential for possible applications, where the ratio between the length of the terminal transient phase and the relevant timescale of the dynamics may probably be crucial when a reasonable prediction (thus a sufficient time before) the end of the chaotic episode is required.

DOI: 10.1103/PhysRevE.98.022215

I. INTRODUCTION

Chaotic dynamics can, in general, be distinguished between persistent chaos and transient chaos, where in the first case the dynamics is mathematically governed by a chaotic attractor. In the latter case, a chaotic saddle is often the underlying state space structure [1,2]. Chaotic transients appear in diverse fields, e.g., in population dynamics [3], coupled FitzHugh-Nagumo oscillators [4], NMR-lasers [5], complex networks [6], cardiac dynamics [7], or may be relevant for plankton blooms [8]. The transition between the chaotic regime and the final attractor is of high interest for many reasons, in particular regarding the potential control of the dynamics. Often, the upcoming self-termination of the chaotic dynamics is not visible in conventional observables a reasonable amount of time before the transition. Due to the chaotic nature of the dynamics, also data assimilation techniques aiming at predicting the dynamics of chaotic systems are limited. Therefore, it is not clear whether a prediction of the end of a chaotic episode is in principle possible a (reasonable) amount of time before. However, in Ref. [9] it was shown in spatially extended systems and low-dimensional map that the transition from the chaotic regime toward the (nonchaotic) attractor of the system is a process with a finite length, called "terminal transient phase" (TTP), which becomes manifest in a change of the state space structure.

In this study, we investigate whether the TTP can be observed also in other models and is therefore a robust phenomenon of chaotic transients in general. In particular, we investigate the spatially extended Gray-Scott model, and the two-dimensional Hénon map. Furthermore, we are interested how the length of the TTP changes if quantities like the system size or model parameters are changed. This investigation is a step toward a better understanding of the transition process from the chaotic dynamics toward the final attractor and promotes in this way the development of possible applications in the future.

This article is structured in the following way: In the first section we introduce the models discussed in this study (Gray-Scott model, Hénon map, tent map). To clarify the procedure which we use to determine the length of the TTP, the approach is explained stepwise in the next section. We demonstrate in the following part that a finite TTP exists also in the models we investigate here, and we compare the length of the TTP to the Lyapunov time. In the subsequent section we investigate how the length of the TTP behaves under changes of the system size (Gray-Scott model) and parameter changes (Hénon map and tent map) and discuss our results in the last section.

II. MODELS

A. Gray-Scott model

The Gray-Scott model [10] is a simple system of partial differential equations which model a chemical reaction of

*thomas.lilienkamp@ds.mpg.de

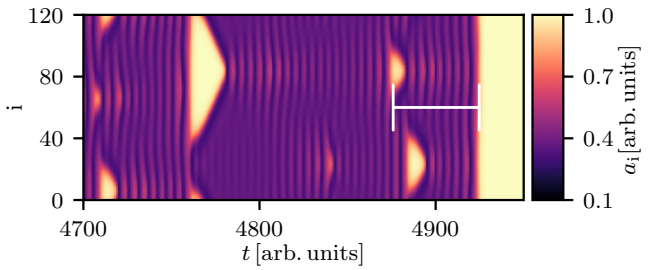

FIG. 1. Exemplary episode of a chaotic transient based on simulations of the Gray-Scott model on a one-dimensional ring with N = 120 elements. Variable a_i (reactant A) is depicted for the final part of this episode just before self-termination (at around $t_{\text{term}} = 4925$ arb. units). The white bar depicts a rough estimate of the length of the terminal transient phase, which is calculated based on an average over many different trajectories, discussed later in this manuscript.

the species U, V, and P: $U + 2V \to 3V$, $V \to P$. It can exhibit diverse irregular spatiotemporal patterns [11] and its features of transient chaos have been studied by Wackerbauer *et al.* [12]. The model equations describe the evolution of the concentrations a_i and b_i of the chemical species U and V in element i, respectively [Eqs. (1) and (2)], where both variables are diffusive (first terms, respectively):

$$\frac{\partial a_i}{\partial t} = D\Delta a_i + 1 - a_i - \mu a_i b_i^2, \tag{1}$$

$$\frac{\partial b_i}{\partial t} = D\Delta b_i + b_0 - \Phi b_i + \mu a_i b_i^2. \tag{2}$$

Our simulations were performed on a one-dimensional ring, using a diffusion constant of $D = 16$, a spacing constant of $h = 1$ and a time constant of $dt = 0.005$, where periodic boundary conditions were used. The following choice of parameters was used: $\mu = 33.7$, $\Phi = 2.8$, and $b = 0$. The one-dimensional simulation domain was initialized with $a = 1$ and $b = 0$. Chaotic dynamics was then induced by setting the b variable at three blocks of each three nodes to one. The three blocks had a minimal distance of 18 nodes. An example of a chaotic episode and the following self-termination of the dynamics is shown in Fig. 1. A periodic dynamic can be observed (with a period of around 5 or 6 arb. units) interrupted by areas of various sizes of a high concentration (e.g., around $t = 4760$), which after their appearance decrease in their size and disappear.

B. Hénon map

The Hénon map [13] is a two-dimensional invertible map, defined by Eqs. (3) and (4):

$$x_{n+1} = a + by_n - x_n^2\,, \tag{3}$$

$$y_{n+1} = x_n\,. \tag{4}$$

In this study, we use $b = 0.3$ and varied the parameter a to achieve transient chaos. Osinga [14] showed how a boundary crisis bifurcation leads to transient chaos in this system [14–16], where in a certain parameter regime, the chaotic attractor collides with the boundary of its basin. Figures 2(a) and 2(b) depict such a transition. In subplot (a) for $a = 1.4$, the chaotic attractor (red) can be determined by the unstable manifold of a fixed point P_1 [blue dot in (a)], whereas the boundary of the basin of the attractor (green) is given by the stable manifold of a second fixed point P_2. With a parameter value of $a = 1.428$, the boundary crisis has taken place [Fig. 2(b)] and the unstable manifold of P_1 touches the stable manifold of P_2 at infinitely many points. Initial conditions (x_0, y_0) were created by a homogeneous randomized distribution on the two-dimensional domain $-3 < x < 3$ and $-3 < y < 3$.

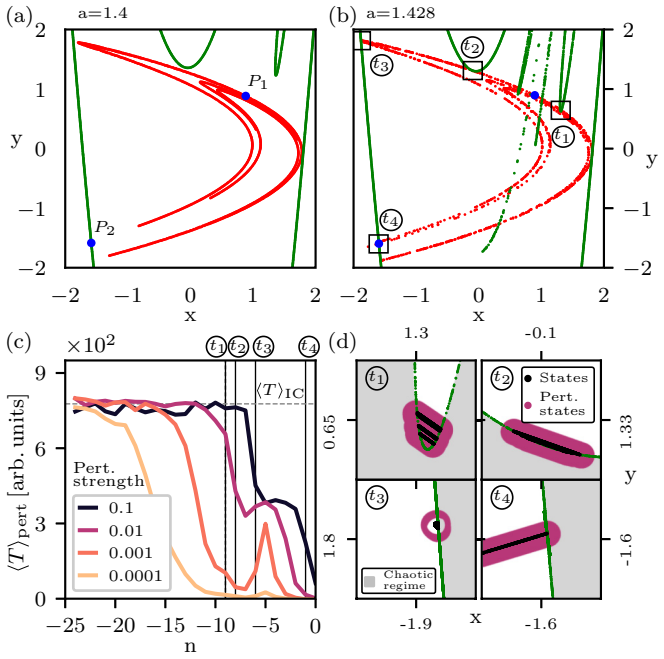

FIG. 2. The terminal transient phase in the Hénon map. Subplots (a) and (b) depict the boundary crisis bifurcation which enables the transient dynamics. In (a) ($a = 1.4$), the attractor of the system (red) is described by the unstable manifold of the fixed point P_1, whereas its basin is determined by the stable manifold of the fixed point P_2. In (b) ($a = 1.428$), the attractor has collided with its own basin. $\langle T\rangle_{\text{pert}}$ is shown in (c) for various perturbation amplitudes. Specific regions of the state space (marked by (t_1)–(t_4) in (b) and (c)) are magnified in subplot (d), each plot with a size of (0.1, 0.1). Trajectories pass these regions before the self-termination. The distribution of the trajectories before the collapse are marked in black in subplot (d), whereas the distribution of the trajectories after the application of a perturbation of strength $\Delta = 0.01$ (corresponding to the purple line in (c)) is marked in purple. The gray-shaded region denotes here the chaotic regime of the state space. Trajectories which are perturbed toward the gray region remain (at least for the moment) chaotic. Thus, by geometrical considerations the overlap of the gray and the purple domains does roughly estimate the probability, that a perturbation can prevent the trajectory from the collapse.

C. Tent map

The tent map is a simple one-dimensional map, described by

$$x_{n+1} = \begin{cases} a_{\text{tent}} x_n & \text{for } x < \frac{1}{2} \\ a_{\text{tent}}(1 - x_n) & \text{for } x \geqslant \frac{1}{2}\,, \end{cases} \tag{5}$$

with the parameter a_{tent}. When a_{tent} is increased above 1.0 (green dashed line), an "exit" from the chaotic regime is formed. This exit window then enables the transient dynamics. The terminal transient phase of the tent map can be determined analytically, as discussed in Ref. [9].

III. DETERMINATION OF THE AVERAGE LIFETIME AND THE TTP

A. Average Lifetime $\langle T \rangle_{\text{IC}}$

The average lifetime is an important quantity which can be used to characterize the chaotic transients which we investigate in this study. It can be determined by creating many initial conditions, which show chaotic dynamics. In this study, 10 000 initial conditions were used for each model. When evolving the initial conditions for a certain amount of time, some fraction of the initial 10 000 trajectories have self-terminated and do not show chaotic behavior anymore.

In the case of the Gray-Scott model, the collapse of the chaotic dynamics was defined when the mean of the variable a_{i}, averaged over the whole simulation domain was above a threshold $\frac{1}{N}\sum_i a_i > 0.99$. In the case of the Hénon map, trajectories that leave the chaotic regime run through specific regions in the state space. After passing a small domain around $(x, y) \approx (-1.91, 1.8)$ [Fig. 2(d) (t_3)], the trajectories diverge to negative infinity [Fig. 2(d) (t_4)]. Thus, the range in time when trajectories terminated could in a first step be identified, when they pass the mentioned regions in state space. The exact definition of the point of termination was then chosen as the beginning of the divergence to negative infinity [one step after passing $(x, y) \approx (-1.91, 1.8)$].

The quantity $N_{\text{Ch}}(t)$, with $N_{\text{Ch}}(t = 0) = 10\,000$ describes the number of initial conditions, which exhibit chaotic dynamics at time t. Typically, this quantity decreases exponentially $N_{\text{Ch}}(t) \sim \exp(-\kappa\, t)$, with the escape rate κ which is approximately inverse to the average lifetime $\kappa \approx \frac{1}{\langle T \rangle}$. In this way, the average lifetime $\langle T \rangle_{\text{IC}}$ can be determined via fitting $N_{\text{Ch}}(t)$ and extracting κ. For the determination of $\langle T \rangle_{\text{IC}}$, the amount of time equal to 500 time units (Gray-Scott model) were discarded. The subscript IC emphasizes that the average lifetime is determined here based on different initial conditions. This procedure is also discussed in Refs. [1,7].

The average lifetime $\langle T \rangle_{\text{IC}}$ depends both, on the choice of parameters of the respective model (e.g., Hénon map), and also on the size of the system (Gray-Scott model). This dependence will also be discussed in the next sections.

B. The length of the TTP

The terminal transient phase is the central quantity investigated in this study, which was introduced in Ref. [9]. The procedure of determining the length of the TTP of a system which exhibits chaotic transients can be divided into the following steps:

(1) Choose a (reference) trajectory $s(t)$ and determine the point in time of self-termination t_{term}.

(2) Determine the state of the chosen trajectory, at a specific time step t_{step} before self-termination, $s(t_{\text{term}} - t_{\text{step}})$.

(3) Apply single perturbations (of a chosen amplitude/strength Δ) to the state $s(t_{\text{term}} - t_{\text{step}})$. The number of independent perturbations is determined by the dimensionality d of the system. This results in d perturbed states.

(4) Evolve these perturbed states until each trajectory has self-terminated.

(5) Measure the lifetimes T_{i} of the perturbed trajectories, where $\text{i} \in \{1, ..., d\}$, starting from the point in time, when the perturbations were applied.

(6) Calculate the mean lifetime, averaged over all perturbed trajectories $\langle T \rangle_{\text{pert}} = \frac{1}{d}\sum_{\text{i}} T_{\text{i}}$. Remember that this quantity corresponds to the specific point in time $t_{\text{term}} - t_{\text{step}}$, and a specific state of the original (reference) trajectory $s(t_{\text{term}} - t_{\text{step}})$.

(7) Repeat steps (2)–(6) by choosing other points in time before self-termination (multiples of t_{step}), thus going stepwise back in time.

Typically, when perturbing the reference trajectory at points close to its self-termination, $\langle T \rangle_{\text{pert}}$ is close to zero. Thus, almost no perturbation can prevent the upcoming self-termination. If perturbations are applied further away from the self-termination of the reference trajectory, $\langle T \rangle_{\text{pert}}$ typically increases (on average), and at some point it will saturate at the average lifetime $\langle T \rangle_{\text{IC}}$ based on different initial conditions. At this point, the state does not show a significant correlation to the upcoming self-termination anymore (regarding the applied finite perturbations). The temporal length starting from the point in time where $\langle T \rangle_{\text{pert}}$ saturates at $\langle T \rangle_{\text{IC}}$ until the self-termination of the reference trajectory, is denoted as the length of the TTP.

Since, in general, $\langle T \rangle_{\text{pert}}$ based on only one trajectory fluctuates, it is necessary to repeat the procedure above with more than one reference trajectory and average $\langle T \rangle_{\text{pert}}$ over these trajectories, where time is normalized regarding the points in time of self-termination of each trajectory. In these cases, $\langle T \rangle_{\text{pert}}$ includes the average over lifetimes of perturbed trajectories which are related to a specific reference trajectory, and a subsequent average over different reference trajectories.

IV. TTP IN THE GRAY-SCOTT MODEL AND THE HéNON MAP

A. Gray-Scott model

Using the procedures discussed in the last section, we investigated a typical trajectory of the Gray-Scott model with $N = 120$ elements (example from Fig. 1).

The analysis is shown in Fig. 3. In a first step, the average lifetime $\langle T \rangle_{\text{IC}}$ of chaotic transients [sketched as the dashed gray line in Fig. 3(a)] was determined based on 10 000 initial conditions. $\langle T \rangle_{\text{pert}}$ was then determined for various perturbation strengths ($\Delta \in [1.0,\ 0.1,\ 0.01,\ 0.001]$), shown in Fig. 3(a) in different colors. As mentioned before, when the point in time when the perturbations are applied is close to self-termination of the reference trajectory (here at around $t_{\text{term}} = 4925$ arb. units, marked by the black arrow), $\langle T \rangle_{\text{pert}}$ is close to zero. When going back in time, however, $\langle T \rangle_{\text{pert}}$ increases and saturates at some point at $\langle T \rangle_{\text{IC}}$. In contrast to (for example) the Fenton-Karma model (discussed in Ref. [9]), the point in time of this saturation depends on the amplitude Δ of the perturbation. By applying a perturbation with a

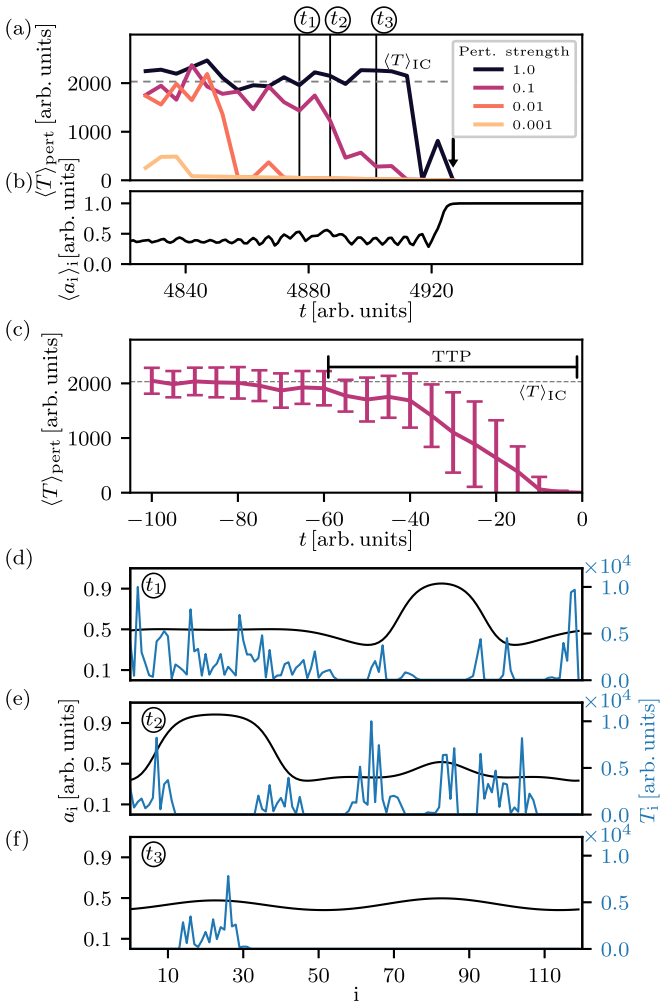

FIG. 3. The terminal transient phase in the Gray-Scott model. An exemplary trajectory (self-termination at approximately $t_{\mathrm{term}} = 4925$) is investigated in subplot (a). $\langle T\rangle_{\mathrm{pert}}$ is shown for different perturbation strengths in different colors. As a comparison, the first variable averaged over the whole domain $\langle a\rangle_i$ does not show obvious indications for the upcoming self-termination a significant amount of time in advance. In (c) $\langle T\rangle_{\mathrm{pert}}$ is sketched for a fixed perturbation strength of $\Delta = 0.1$, averaged over 50 trajectories, where time is normalized such that self-termination happens at $t = 0$. The temporal length of the TTP can in this way be estimated (TTP $\approx$ 60 arb. units). The length of the TTP is sketched as the black bar, where the end of the TTP is determined by the end of the chaotic dynamics ($t = 0$), and the beginning can be roughly estimated as the point, where $\langle T\rangle_{\mathrm{pert}}$ saturates at $\langle T\rangle_{\mathrm{IC}}$. Snapshots of the first variable a_i of the trajectory discussed in subplot (a) are shown in black in subplots (d), (e), and (f) [corresponding to three points in time t_1, t_2, and t_3, which are additionally marked as black vertical lines in subplot (a)]. The transient times T_i corresponding to perturbations applied at the ith element of the system at the respective point in time are shown in blue in (d), (e), and (f), for the three points in time, respectively. Connected regions in the i space are visible, where the transient lifetimes that correspond to perturbations are close to zero (e.g., at t_2 around $10 < i < 30$). These regions constitute an increasing part of the whole space, as the point in time when the perturbations are applied comes closer to the point of self-termination of the original trajectory.

larger amplitude, the chance of preventing the upcoming self-termination is higher.

This analysis demonstrates that the state space structure in the vicinity of the reference trajectory changes already a finite amount of time before its self-termination. Nevertheless, this "transition" is not visible in conventional variables, as, for example, the spatial mean $\langle a_i\rangle_i$ [shown in Fig. 3(b)]. The temporal length of this transition zone can be estimated by the distance from the point in time where $\langle T\rangle_{\mathrm{pert}}$ saturates at $\langle T\rangle_{\mathrm{IC}}$ and the time of self-termination. As stated before, the saturation point depends on the strength of the applied perturbations. For an estimate of the length of the TTP we chose here a perturbation strength of $\Delta = 0.1$ and determined $\langle T\rangle_{\mathrm{pert}}$ for 50 trajectories [average shown in Fig. 3(c)]. Based on this expression, one can estimate the length of the TTP (regarding the specific perturbation strength) of around TTP $\approx$ 60 arb. units.

Investigating the spatial distribution of lifetimes T_i (the lifetime of the trajectory which originates from perturbing the reference trajectory at the node i) provides a first insight into the underlying mechanism. T_i is shown for the example trajectory [Fig. 3(a)] in Figs. 3(d), 3(e) and 3(f) in blue for three different points in time t_1, t_2, and t_3 before self-termination. The points in time are additionally marked in Fig. 3(a) with black vertical lines. The black lines in Figs. 3(d), 3(e) and 3(f), respectively, show snapshots of the state variable a_i at the respective points in time. The lifetimes T_i depend in an irregular pattern on the spatial position i, which is typical for a chaotic dynamic. Furthermore, spatially connected regions establish with a lifetime close to zero (e.g., at t_2 around $i = 15$), which grow over time such that at t_3 T_i is nonzero only in a spatially confined region.

That means, when the reference trajectory comes closer to its self-termination, less perturbations can significantly change the trajectory and prevent the upcoming self-termination. In this way, probing the vicinity of the reference trajectory with small perturbations reveals a specific structure of the state space and suggests the picture of high-dimensional tubes which determine the dynamics at the "exits" of the chaotic regime. As a remark, using spatially localized perturbations (corresponding to orthogonal coordinate axes) enabled the observation of the spatially connected regions discussed above. Using the more general choice of arbitrary n balls as perturbations (which we actually use in the next section in the case of the Hénon map) would have made this insight considerably more difficult.

To emphasize the conceptual difference between the investigations shown in this study (using small but finite perturbations) and the concept of a Lyapunov analysis, we compare the length of the TTP with the Lyapunov time $t_{\mathrm{L}} = 1/\lambda_1$ (with λ_1 the largest Lyapunov exponent, computed during the chaotic transients) which we computed for the system of N = 120 nodes. The difference between the TTP $\approx$ 60 arb. units and the Lyapunov time of $t_{\mathrm{L}} \approx 5.08$ arb. units underlines that the information obtained by our analysis provides additional insight into the state space structure.

B. Hénon map

The second model we investigate here is the two-dimensional Hénon map. Since it is lower dimensional than,

e.g., the spatially extended system of the Gray-Scott model discussed before, possible mechanisms can be understood in a more intuitive way. As stated before, transient chaotic dynamics can be induced via a boundary crisis bifurcation by adjusting the parameter a [Figs. 2(a) and 2(b)]. Using 10 000 initial conditions, the average lifetime $\langle T\rangle_{\mathrm{IC}}$ of the transients was determined as described before.

$\langle T\rangle_{\mathrm{pert}}$ was determined by applying perturbations to 10 000 trajectories. The perturbations are two-dimensional (x, y), in random directions, but with a constant perturbation amplitude Δ. In Fig. 2(c) $\langle T\rangle_{\mathrm{pert}}$ is shown for different amplitudes. The terminal transient phase can also be recognized in this model, with a length of approximately TTP ≈ 12 steps (concerning a perturbation strength of $\Delta = 0.01$), which is significantly larger than the Lyapunov time of $t_{\mathrm{L}} \approx 2.3$ steps.

Furthermore, we found that all trajectories are passing relatively small areas in the state space before their termination. These regions of the state space [marked by (t_1)–(t_4) in Fig. 2(b)] are magnified in Fig. 2(d). Trajectories pass these regions at 9 (t_1), 8 (t_2), 6 (t_3), and 1 (t_4) steps before self-termination, respectively [also marked as vertical dashed lines in Fig. 2(c)]. In the enlarged maps of the state space [Fig. 2(d)], the distribution of the states of 10 000 trajectories is depicted in black. Although the chaotic attractor does not exist anymore here, the stable manifold of the fixed point P_2 still determines the boundary between chaotic (gray-shaded) and nonchaotic domains of the state space. The area colored in purple sketches the region where the trajectories are distributed after a perturbation of amplitude $\Delta = 0.01$ [corresponding to the purple line in subplot (c)]. The behavior of $\langle T\rangle_{\mathrm{pert}}$ can be understood here using an intuitive geometrical picture: The overlap of the purple area (perturbed trajectories) and the gray-shaded region of the state space (chaotic regime) is a good approximation for the amount of trajectories that remain after the perturbation inside the chaotic regime (prevention of the collapse). This is in particular plausible for the case $n = -1$ [(t_4), thus trajectories which are one step away from self-termination], where only few trajectories can be perturbed back toward the chaotic regime. Also, the difference of $\langle T\rangle_{\mathrm{pert}}$ between different perturbation amplitudes at $n = -9$ (t_1), thus trajectories which will self-terminate in nine steps) is reasonable in this picture when referring to subplot (d, t_1): perturbations of size $\Delta = 0.01$ (purple curve) can shift a significant amount of the trajectories back to the chaotic regime, however, if the perturbation strength decreases (e.g., $\Delta = 0.001$) perturbations are too small to overcome the distance of most of the trajectories (black) to the (former) basin boundary (green), thus, they cannot be perturbed toward the chaotic regime again and self-termination is almost certain. This dynamic is reflected in the difference of $\langle T\rangle_{\mathrm{pert}}$ at t_1 between a perturbation amplitude of $\Delta = 0.001$ and $\Delta = 0.01$ [orange and purple line in Fig. 2(c), respectively].

Furthermore, the characteristic "knee" visible in Fig. 2(c) for $n \geqslant -7$ and perturbation strengths of $\Delta \geqslant 0.01$ can be understood using geometrical considerations. For $n < -7$, the decrease of $\langle T\rangle_{\mathrm{pert}}$ is determined by the change of the curvature of the boundary [e.g., t_1 and t_2 in Fig. 2(d)]. For $n \geqslant -7$, the trajectories are located close to rather straight boundaries [e.g., t_3 in Fig. 2(d)] where the curvature does not change significantly anymore for increasing n. In the final phase ($n \geqslant -5$), the trajectories depart (approximately orthogonally) from the boundary [e.g., t_4 in Fig. 2(d)], which causes the final decrease of $\langle T\rangle_{\mathrm{pert}}$.

The geometrical considerations that provide an intuitive understanding of the mechanism which underlies the formation of the TTP in the Hénon map can be used to interpret the state space structure also in the high-dimensional models, as the Gray-Scott model. Connected regions where perturbations do not significantly change the reference trajectory anymore [see Figs. 3(d), 3(e) and 3(f)] are growing in size when converging to the point of self-termination. This behavior suggests, that similar geometrical or topological structures found in the Hénon map are also present in the state space of high-dimensional models as, for example, the Gray-Scott model.

V. SCALING PROPERTY OF THE LENGTH OF THE TTP

In this section we investigate how the length of the TTP depends on (i) the system size and (ii) choice of parameters of the respective model. For this purpose, we (i) vary the number of elements of the one-dimensional ring of Gray-Scott simulations and we (ii) modify parameter a of the Hénon map, which was adapted in Ref. [14] to cause the boundary crisis.

In the first case we determine the average lifetime $\langle T\rangle_{\mathrm{IC}}$ of chaotic transients for a various number of elements N ([120, 130, 140, 150, 160]) and find that $\langle T\rangle_{\mathrm{IC}}$ is increasing exponentially with the system size [black dots in Fig. 4(b)]. This behavior can be observed in a whole group of spatially extended systems which exhibit chaotic transients (e.g., Ref. [17]), called type-II transient turbulence [18] or type-II supertransients [1].

In the Hénon map the average lifetime $\langle T\rangle_{\mathrm{IC}}$ depends sensitively on the choice of parameter a [black dots in Fig. 4(d)]. Indeed, below $a \approx 1.4269212$ the boundary crisis does not happen and persistent chaos can be observed. Reducing parameter a from above this bifurcation point increases the average lifetime $\langle T\rangle_{\mathrm{IC}}$ until the dynamics is governed by a chaotic attractor. This dependence of the transient lifetime on a critical parameter p has been investigated in the vicinity of a critical point p_{crit} for various systems, e.g., in Refs. [19,20], where it was shown that

$$\langle T\rangle_{\mathrm{IC}} \sim (p - p_{\mathrm{crit}})^{-\gamma}, \tag{6}$$

with a critical exponent γ, which is $\gamma = 2$ in the case of the Hénon map. This transition from transient chaos to persistent chaotic dynamics has, however, not been reported for the Gray-Scott model where the average lifetime merely grows exponentially.

Regarding this sensitive dependence of the timescale of $\langle T\rangle_{\mathrm{IC}}$ on the spatial size of the system and the choice of parameters, we are interested how the temporal length of the TTP scales under this conditions. Beyond calculating the average lifetime of chaotic transients [black dots in Figs. 4(b) and 4(d), respectively, for the Gray-Scott model and the Hénon map], the length of the TTP was determined for each system size and choice of parameter a, respectively, using a fixed perturbation amplitude of $\Delta = 0.1$ (Gray-Scott model) and $\Delta = 0.01$ (Hénon map). $\langle T\rangle_{\mathrm{pert}}$ (normalized by the respective

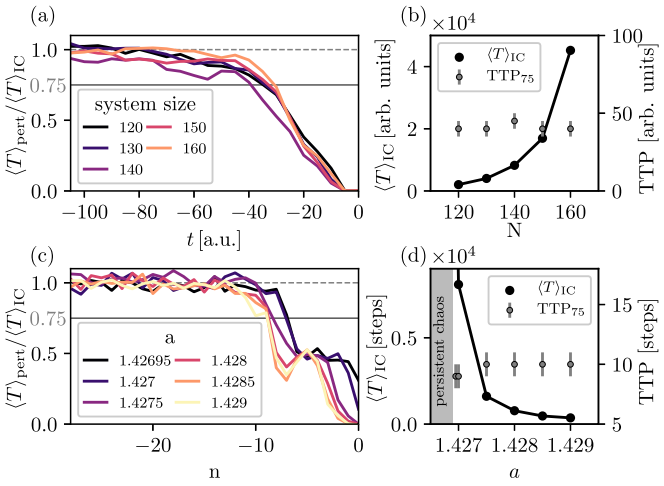

FIG. 4. The scaling property of the length of the TTP. In subplot (a), $\langle T\rangle_{\mathrm{pert}}$ is shown (normalized to $\langle T\rangle_{\mathrm{IC}}$) for varying system size (indicated by the color) for the Gray-Scott model. Each curve is calculated based on 50 trajectories. The dependence of $\langle T\rangle_{\mathrm{IC}}$ on the system sizes is depicted in subplot (b), separately (in black). To compare the length of the TTP for different system sizes, the point in time is determined for each curve where $\langle T\rangle_{\mathrm{pert}}$ reaches 75% of $\langle T\rangle_{\mathrm{IC}}$. This quantity TTP$_{75}$ is shown in (b) for each system size. The same analysis has been performed for the Hénon map in subplots (c) and (d), where $\langle T\rangle_{\mathrm{pert}}$ and $\langle T\rangle_{\mathrm{IC}}$ have been determined for varying parameter a. The gray-shaded region in subplot (d) indicates the parameter regime where the chaotic dynamics is persistent. In the Gray-Scott model and the Hénon map, the average lifetime of chaotic transients depends sensitively on the system size (b) or the parameter a (d), respectively. However, the length of the TTP measured by TTP$_{75}$ does not change significantly.

average lifetime $\langle T\rangle_{\mathrm{IC}}$) is shown for each system size in Fig. 4(a) (Gray-Scott model) and each choice of parameter a in Fig. 4(c) (Hénon map).

To achieve a reasonable comparison of the length of the TTP between the different cases, we measured the point in time when $\langle T\rangle_{\mathrm{pert}}$ reaches 75% of the average transient lifetime $\langle T\rangle_{\mathrm{IC}}$ (denoted as TTP$_{75}$). With this approach we reduce the influence of fluctuations of $\langle T\rangle_{\mathrm{pert}}$, which originate from the finite number of reference trajectories investigated (50 in the case of Gray-Scott model, 10 000 in the case of the Hénon map). TTP$_{75}$ is sketched in Figs. 4(b) and 4(d), respectively, as gray dots. Small variations can be observed, dependent on the system size (Gray-Scott model) and the parameter a (Hénon map), respectively, but no clear trend is visible. That means, although the average lifetime of both systems changes by orders of magnitude, the length of the TTP remains relatively constant.

Despite these empirical investigations, in the tent map the change of the length of the TTP due to parameter changes can be determined analytically. As described in Ref. [9], the transient lifetime depends on the only parameter of the map a_{tent}, where for $0 < a_{\mathrm{tent}} \leqslant 2$ persistent chaos can be observed whereas for $a_{\mathrm{tent}} > 2$ the chaotic dynamics is transient within the unit interval (0, 1).

The following considerations regarding the analytical determination of the TTP in the tent map have been discussed in

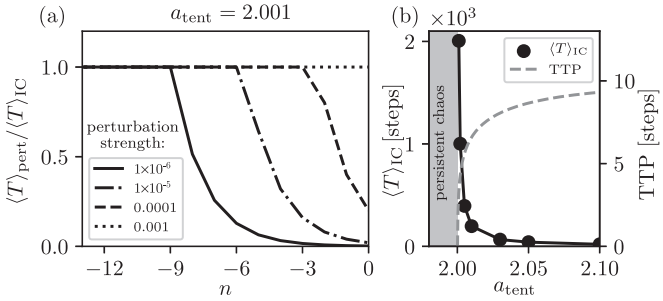

FIG. 5. The TTP in the tent map. $\langle T\rangle_{\mathrm{pert}}$ (normalized to $\langle T\rangle_{\mathrm{IC}}$) is shown in subplot (a) for different perturbation strengths [based on Eq. (7)] and a fixed parameter $a_{\mathrm{tent}} = 2.001$. In subplot (b), the average lifetime $\langle T\rangle_{\mathrm{IC}}$ is sketched in black for a varying parameter a_{tent}. Also, the length of the TTP which is determined based on Eq. (10) for a fixed perturbation strength of $\Delta = 0.0001$ is depicted as the gray dashed line. The gray-shaded region indicates the regime where the chaotic dynamics is persistent.

Ref. [9]. Here, $\langle T\rangle_{\mathrm{pert}}$ can be determined analytically:

$$\langle T\rangle_{\mathrm{pert}}(n, \Delta) = \langle T\rangle_{\mathrm{IC}} \min\left(\frac{\Delta}{L(n)}, 1\right), \tag{7}$$

$$L(n) = (a_{\mathrm{tent}} - 2)/a_{\mathrm{tent}}^{-n}, \tag{8}$$

with $n \in [-1, -2, -3, \dots]$. Using Eq. (7), $\langle T\rangle_{\mathrm{pert}}$ can be determined for different perturbation amplitudes (sketched (normalized to $\langle T\rangle_{\mathrm{IC}}$) in Fig. 5(a), with $a_{\mathrm{tent}} = 2.001$).

Consequently, the length of the TTP is defined by the following equation:

$$\frac{\Delta}{L(n)} = 1, \tag{9}$$

which results in the dependence between n and a_{tent},

$$n_{\mathrm{TTP}}(a_{\mathrm{tent}}) = -\log_{a_{\mathrm{tent}}} \frac{a_{\mathrm{tent}} - 2}{\Delta}. \tag{10}$$

Based on Eq. (10), the length of the TTP is sketched in Fig. 5(b) (gray dashed line) for a perturbation amplitude of $\Delta = 0.0001$ together with $\langle T\rangle_{\mathrm{IC}}$ (which was calculated based on 10 000 initial conditions). Initial conditions were chosen randomly from the unit interval (0, 1). The self-termination of the chaotic dynamics was defined, when a value >1 was reached.

Similar to the analysis of the Hénon map, the transient lifetime increases as the parameter a_{tent} approaches the "boundary" between persistent and transient chaos (at $a_{\mathrm{tent}} = 2$). Also here, the average lifetime $\langle T\rangle_{\mathrm{IC}}$ can be described close to $a_{\mathrm{tent}} = 2$ by Eq. (6) with $\gamma = 2$.

At the same time, the length of the TTP drops significantly in this region. Since it grows logarithmically with increasing a_{tent}, for larger a_{tent} it will not change dramatically.

If the underlying mechanism which causes the appearance of the TTP based on the state space structure is comparable to the Hénon map, the dependence of the length of the TTP on parameter changes (here controlling the "distance" to the regime of persistent chaos) should also be similar. From this perspective, the drop of TTP$_{75}$ in Fig. 4(d) around $a = 1.427$ could be an indication for comparability. However, we could not verify this conjecture, or validate a general scaling behavior.

VI. CONCLUSION

In this study we investigated the terminal transient phase of chaotic transients in a spatially extended domain of the Gray-Scott model, and the two-dimensional Hénon map. A terminal transient phase of finite size could be determined in both models, emphasizing the generality of this phenomenon (additional to the Fenton-Karma model [21], the Morris-Lecar network [22], and the tent map, discussed in Ref. [9]). Furthermore, we showed that the temporal length of the TTP is substantially longer than the Lyapunov time. This underlines that the approach of probing the state space with small but finite perturbations provides different insight into the structure of the state space than the Lyapunov approach, which characterizes the evolution and impact of infinitesimally small perturbations, only. The terminal transient phase is a robust feature occurring in many systems (of various complexity and dynamics) which exhibit chaotic transients. So far, it cannot be understood using "conventional" methods from nonlinear dynamics (e.g., Lyapunov analysis). For a dynamical system like the tent map where all local Lyapunov exponents are the same (homogeneous stretching behavior) the Lyapunov exponent(s) characterize(s) the growth rate of the exit sets (as long as the size of these sets does not exceed some limit of the linear approximation underlying the concept of Lyapunov exponents). In the general case, where local Lyapunov exponents may fluctuate (significantly) the link between (globally averaged) Lyapunov exponents and the local stretching properties of the exit sets is not so obvious. If the exit sets are distributed on the chaotic saddle in a way such that the average of the local stretching at the exit sets is close to the value of the (global) Lyapunov exponents then the Lyapunov exponents might be used to characterize the lengths of the TTP. However, whether and when this condition is fulfilled is not clear *a priori*.

We furthermore investigated how the length of the TTP depends on parameter changes and system size variations, which in the models discussed in this study resulted in a significant shift of the average transient lifetime of the chaotic transients. In the Gray-Scott model, a change of the length of the TTP could not be detected, although the average lifetime of the chaotic transients increased by orders of magnitude when increasing the size of the spatial domain. Also in simulations of the Hénon map, changing a model parameter did not notably affect the length of the TTP. However, analytical investigations of the tent map indicated a parameter dependent length of the TTP that decreased logarithmically when approaching the parameter value of persistent chaos ($a_{\text{tent}} = 2$). Whether the underlying mechanisms of the TTP in the tent map and in the Hénon map are comparable is nevertheless not clear.

Additional to the analytical considerations regarding the emergence of the TTP in the tent map, the appearance of the TTP in the Hénon map can at least be understood geometrically by observing trajectories in the state space. In particular, the boundary between the chaotic and the nonchaotic regime in the state space could be determined, and the shape or curvature of the boundary in the vicinity of trajectories improves the understanding for the underlying mechanism. Spatially connected regions of perturbations which cannot prevent the upcoming self-termination in simulations of the Gray-Scott model suggest that the change of the state space structure which causes the creation of the TTP may be comparable.

Since the timescale of the length of the TTP may be essential in applications, the fact that the temporal length of the TTP does not depend sensitively on the choice of parameters or the size of the system (at least in the models studied here) could be practically relevant. In particular when one is interested in predicting the upcoming self-termination, the length of the TTP needs to be compared to the relevant timescale of the specific system. For example, the terminal transient phase of the transient chaotic dynamics of spiral waves as a model for ventricular fibrillation should be equal or larger than the intrinsic timescale of the system, which is here the spiral period. If the length of the TTP does not (or only weakly) depend on the system size or parameters, a prediction of self-termination of the chaotic dynamics in the heart could in principle be possible, based on the features of the terminal transient phase.

The end of the transients regarding the models we investigated so far was mainly abrupt, thus, the transient lifetimes could be determined in a rather straightforward manner. In general, determining the end of transient dynamics can be nontrivial. To investigate cases of nonabrupt self-termination (for example, if the attractor is reached via weakly damped oscillations) suitable criteria are required for determining the moment in time when the attractor is reached, like those presented and investigated by Kittel *et al.* [23] for the general problem of quantifying reaching times.

ACKNOWLEDGMENTS

We thank the International Max Planck Research School (IMPRS) for Physics of Biological and Complex Systems (PBCS), the Federal Ministry of Education and Research (BMBF, FKZ031A147, GO-Bio), and the Collaborative Research Center SFB937 (DFG) "Collective Behavior of Soft and Biological Matter" for financial support. Furthermore, we thank Stefan Luther for fruitful discussions and continuous support.

[1] Y.-C. Lai and T. Tél, *Transient Chaos: Complex Dynamics on Finite Timescales*, in Applied Mathematical Sciences Vol. 173 (Springer, New York, 2011).

[2] Y.-C. Lai and R. L. Winslow, Phys. Rev. Lett. **74**, 5208 (1995).

[3] K. McCann and P. Yodzis, Am. Nat. **144**, 873 (1994).

[4] G. Ansmann, K. Lehnertz, and U. Feudel, Phys. Rev. X **6**, 011030 (2016).

[5] I. M. Jánosi, L. Flepp, and T. Tél, Phys. Rev. Lett. **73**, 529 (1994).

[6] A. Zumdieck, M. Timme, T. Geisel, and F. Wolf, Phys. Rev. Lett. **93**, 244103 (2004).

[7] T. Lilienkamp, J. Christoph, and U. Parlitz, Phys. Rev. Lett. **119**, 054101 (2017).

[8] E. Hernández-García and C. López, Ecological Complexity **1**, 253 (2004).

[9] T. Lilienkamp and U. Parlitz, Phys. Rev. Lett. **120**, 094101 (2018).
[10] P. Gray and S. Scott, Chem. Eng. Sci. **39**, 1087 (1984).
[11] J. E. Pearson, Science **261**, 189 (1993).
[12] R. Wackerbauer and K. Showalter, Phys. Rev. Lett. **91**, 174103 (2003).
[13] M. Hénon, Commun. Math. Phys. **50**, 69 (1976).
[14] H. M. Osinga, J. Dif. Equat. Appl. **12**, 997 (2006).
[15] C. Grebogi, E. Ott, and J. A. Yorke, Physica D: Nonlin. Phenom. **7**, 181 (1983).
[16] T. Tél and M. Gruiz, *Chaotic Dynamics: An Introduction Based on Classical Mechanics* (Cambridge University Press, Cambridge, 2006).
[17] A. Wacker, S. Bose, and E. Schöll, Europhys. Lett. **31**, 257 (1995).
[18] J. P. Crutchfield and K. Kaneko, Phys. Rev. Lett. **60**, 2715 (1988).
[19] C. Grebogi, E. Ott, and J. A. Yorke, Phys. Rev. Lett. **57**, 1284 (1986).
[20] C. Grebogi, E. Ott, F. Romeiras, and J. A. Yorke, Phys. Rev. A **36**, 5365 (1987).
[21] F. Fenton and A. Karma, Chaos **8**, 20 (1998).
[22] C. Morris and H. Lecar, Biophys. J. **35**, 193 (1981).
[23] T. Kittel, J. Heitzig, K. Webster, and J. Kurths, New J. Phys. **19**, 083005 (2017).